Lei Chen, Yean Kee Lee, Yanawut Manmana, Kheng Soo Tay*, Vannajan Sanghiran Lee and Noorsaadah Abd Rahman

Synthesis, characterization, and theoretical study of an acrylamide-based magnetic molecularly imprinted polymer for the recognition of sulfonamide drugs

Abstract: In this work, a magnetic molecularly imprinted polymer (MION-MIP) was prepared for the recognition and extraction of sulfadiazine (SDZ). The acrylamide-based MIP was imprinted directly onto the surface of 3-(trimethoxysilyl)propyl methacrylate-modified magnetic iron oxide nanoparticles. The synthesized MION-MIP with a diameter about 100 nm possesses fast adsorption kinetics and high adsorption capacity. The results also indicated that a higher maximum adsorption capacity (775 μg g^{-1}) was achieved by the synthesized MION-MIP. The Langmuir adsorption isotherm model was found to describe well the equilibrium adsorption data. The results from the competitive binding experiment showed that MION-MIP was not only selective toward SDZ but the adsorption of sulfamerazine was also dramatically high. SDZ and sulfamerazine have an almost similar substructure where these two compounds were only differentiated by one methyl group. To explain this result, a computational study was carried out. From a different level of calculation with semiempirical (PM3), Hartree-Fock (HF), and density functional theory (DFT) calculation, SDZ and sulfamerazine showed similar interaction energy and interaction mechanism with the acrylamide monomer. Therefore, both SDZ and sulfamerazine could have the same binding property with the MION-MIP.

Keywords: adsorption; computer modeling; interaction energy; Langmuir adsorption isotherm model; magnetic iron oxide nanoparticles.

***Corresponding author: Kheng Soo Tay,** Faculty of Science, Department of Chemistry, University of Malaya, 50603 Kuala Lumpur, Malaysia, Tel.: +603-79677022 ext 2145, Fax: +603-79674193, e-mail: khengsoo@um.edu.my
Lei Chen, Yean Kee Lee, Vannajan Sanghiran Lee and Noorsaadah Abd Rahman: Faculty of Science, Department of Chemistry, University of Malaya, 50603 Kuala Lumpur, Malaysia
Yanawut Manmana: Faculty of Science, Department of Chemistry, Prince of Songkla University, Songkhla 90112, Thailand

DOI 10.1515/epoly-2015-0017
Received January 20, 2015; accepted March 12, 2015; previously published online April 14, 2015

1 Introduction

Antibacterial sulfonamides (sulfonamides) are a family of broad-spectrum synthetic bacteriostatic agents used in both human (1) and veterinary medicine (2) for therapeutic purposes. In animal feed, sulfonamides are used to promote livestock growth (3). Among various classes of pharmaceuticals, the presence of antibiotics in the environments has been one of the major concerns due to its ability to develop antibiotic-resistant bacteria (4, 5). Because of their extensive use, sulfonamides have been detected in various environments such as wastewaters, soils, and surface waters. Therefore, the development of a solid phase for the specific extraction of sulfonamides is an important consideration.

Molecular imprinted polymers (MIPs) are polymers containing designed artificial receptors with a predetermined selectivity and specificity for a given analyte (6). Owing to its molecular recognition ability, MIPs have appeared as very promising materials for the separation of target chemicals from different complex matrices such as environmental samples and biological fluids. Recently, various types of MIPs have been used as the adsorbent for solid phase extraction (SPE). These adsorbents have been widely used for the selective separation of various environmental pollutants (7–9), drugs and metabolites (10, 11), as well as bioactive compounds (12–14). Thus far, conventional MIPs are prepared by bulk polymerization or precipitation polymerization (8). These MIPs showed poor binding capacities and low binding kinetics of the target compounds because of the embedded binding sites (15). The application of these conventional MIPs as adsorbents for SPE also involved additional preparation steps, such as crushing and grinding of these polymers into fine

powder followed by SPE cartridge packing (14, 16). The major disadvantage of this conventional SPE is its extraction efficiency that is influenced by the uploading rate of sample and the eluent.

Recently, various approaches have been developed for imprinting MIPs onto the surface of different solid supports (15). This method can enhance the binding capacity of MIPs through the provided high surface area. In this study, acrylamide-based MIP was imprinted onto the surface of magnetic iron oxide nanoparticles (MIONs). MIONs with small particle size have been considered as an ideal solid support that provides a large surface area for adsorption (15). As compared to other solid supports, MIONs offer an added advantage of being magnetically separable, thereby eliminating the requirement of filtration and SPE cartridge packing.

The main objectives of this study were to synthesize acrylamide-based magnetic MIP (MION-MIP) with SDZ as template, and to investigate the adsorption property of MION-MIP toward SDZ. The binding conformation and the interaction between SDZ and acrylamide (monomer) were studied in detail by using computational methods to explain the sulfonamide adsorption. Recently, computational methods have been frequently used in various studies related to MIP (17). However, many studies only applied the computational methods for the selection of the most suitable monomer for MIP preparation based on the interaction between the monomer with the selected template (18–20). In this study, a computational method was used to explain the binding behavior of the synthesized MION-MIP. Based on a literature review, the application of core-shell methacrylic acid-based magnetic MIP for the adsorption of sulfamethazine has been reported by Kong et al. (3). However, in this study, the acrylamide-based MIP was imprinted directly onto the surface of MION; this study has not been reported elsewhere. With this method, MION-MIP with a higher apparent maximum adsorption capacity (Q_{MAX}) was produced.

2 Experimental

2.1 Chemicals

Iron (II) chloride tetrahydrate ($FeCl_2{\cdot}4H_2O$, 99%), iron (III) chloride ($FeCl_3$, 98%), ethylene glycol dimethacrylate (EGDMA, 97.5%), ammonium hydroxide (25%), and all solvents used were purchased from Merck (Germany). 3-(Trimethoxysilyl)propyl methacrylate (MPS, 98%), acetic acid (HAc), and benzoyl peroxide were provided by Sigma (Missouri, USA). Sulfadiazine (SDZ), sulfamerazine (SMR), sulfacetamide (SAA), sulfamethazine (SMZ), and sulfamethoxazole (SMO) were obtained from Alfa Aesar (UK). Acrylamide (98.0%) was supplied by Fluka (Missouri, USA). All chemicals and solvents were used without further purification.

2.2 Preparation of magnetic acrylamide-based nanoparticles

2.2.1 Synthesis of MION-MPS

MION was synthesized by using a coprecipitation method as reported by Karaagac et al. (21). Briefly, $FeCl_2$ and $FeCl_3$ with a molar ratio of 2:3 were first dissolved in 100 ml deionized water. Fifty milliliters of 25% ammonium hydroxide was then added to the mixture of $FeCl_2$ and $FeCl_3$ under vigorous stirring for 30 min, and MION was precipitated by applying an external magnetic field. The collected MION was washed with deionized water and freeze dried.

Surface modification of MION with MPS was performed as follows: 0.2 g dried MION, 0.4 ml MPS, 0.1 ml triethylamine, and 100 ml anhydrous toluene were swirled for 10 min under nitrogen atmosphere. The mixture was refluxed for 36 h under nitrogen atmosphere and vigorous stirring. The MION-MPS was then collected by an external magnetic field, rinsed thoroughly with ethanol six times, and dried under vacuum at room temperature.

2.2.2 Preparation of MION-MIP

SDZ (95 mg) and acrylamide (135 mg) was mixed in 60 ml acetonitrile-toluene with a ratio of 3:1 (v/v), and the mixture was refrigerated for 12 h to form a preassembly solution. Then, MION-MPS (100 mg), EGDMA (1 ml), and benzoyl peroxide (138 mg) were added to the acetonitrile-toluene with a ratio of 3:1 (v/v). The mixture was then degassed for 20 min by sonication and was simultaneously purged by nitrogen gas. Then, the preassembly solution was added through a cannula under nitrogen atmosphere. This combined mixture solution was heated at 50°C for 6 h, 60°C for 24 h, and 85°C for 6 h. After polymerization, the MION-MIP was separated using a magnet and rinsed with methanol. The SDZ (template) in MION-MIP were extracted with methanol-HAc (9:1, v/v). The presence of SDZ in methanol-HAc was determined using high-performance liquid chromatography (HPLC). Finally, the product was repeatedly washed with methanol and dried under vacuum.

The non-imprinted polymer (MION-NIP) was prepared by using the same procedure without SDZ.

2.3 Binding experiments

2.3.1 Binding experiments of MION-MIP and MION-NIP

All biding experiments were carried out at room temperature as described by Kong et al. (3). For the kinetic adsorption experiment, 10 mg of MION-MIP or MION-NIP was added to 3 ml of 10 μg ml^{-1} SDZ solution with acetonitrile as solvent. The mixture was vortexed at regular time intervals ranging from 10 to 1800 s. The MION-MIP or MION-NIP was separated by an external magnetic field, and the concentration of the remaining SDZ in the solution was measured by using HPLC. For the isothermal binding experiment, 10 mg of MION-MIP or MION-NIP were added to 3 ml of SDZ solution with the concentration ranging from 0.50 to 30 μg ml^{-1}. The mixtures were vortexed for 20 min at room temperature. The MION-MIP or MION-NIP was separated from the SDZ solution by an external magnetic field, and the concentration of SDZ in the supernatants was measured by HPLC.

2.3.2 Specific recognition of MION-MIP and MION-NIP

Ten milligrams of MION-MIP or MION-NIP was added to 3 ml acetonitrile containing SDZ, SMZ, SMO, and SMR with a concentration of 10 μg ml^{-1} for each compound. After shaking for 10 min at room temperature, the MION-MIP or MION-NIP was separated from the solution by an external magnetic field, and the concentration of selected sulfonamide supernatants were measured by HPLC.

2.4 Characterization of MION-MIP

Infrared spectra were recorded using a Perkin-Elmer Fourier transform infrared (FTIR) spectrophotometer. The IR spectra of samples were collected in transmission mode by pressing the particle sample with potassium bromide powder to form pellets. A resolution of 2 cm^{-1} and a total of 96 scans were applied for the collection of IR spectra. Thermal gravimetric analysis (TGA) measurements were performed on a TGA4000 Perkin-Elmer instrument. Each sample was heated between 50°C and 800°C (10°C min^{-1}) under air flow (30 ml min^{-1}). The morphology of the MION and MION-MIP was obtained by scanning electron microscopy (SEM) (Hitachi SU8220). Samples were mounted on carbon tape onto aluminum sample holders for analysis.

2.5 Instrumental analysis

All HPLC analyses were performed using a Shimadzu HPLC system consisting of an LC-20AT pump, an SPD-M20A diode array detector, an SIL-20AHT autosampler, a CTO-20AC column oven, and a CBM-20A communication bus module (Shimadzu, Japan). A reversed-phase Supelco Ascentis C18 column (150 mm×4.6 mm; Sigma-Aldrich, USA) was used for separation. The mobile phase was a mixture of acetonitrile and 0.1% formic acid in deionized water. The flow rate was maintained at 1.0 ml min^{-1} for all runs. Isocratic elution was performed with 70% of acetonitrile. The detection wavelength was 258 nm.

2.6 Computational study

Geometrical optimizations for the search of possible interactions between the monomer, acylamide with the templates (SDZ), and SMR were carried out using semiempirical (PM3), *ab initio* (HF/6-31G(d)), and density functional theory (DFT) using Becke's three-parameter Lee-Yang-Par (B3LYP) functional and 6-31G(d) basis set. Then, single point energy calculation was performed on the optimized structure to estimate the interaction energy (ΔE_{int}) between the template and monomer from the equation $\Delta E_{int}=E_{complex}-E_{template}-E_{monomer}$. The optimized structures from the B3LYP/6-31G(d) method have been used for scanning the interaction energy between the SDZ and SMR with the monomer against the distance from -1.000 to +4.000 Å of the distance with the step size of 0.200 Å. All the quantum calculations were performed using Gaussian 09 software.

3 Results and discussion

3.1 Characteristic of MION-MIP

In this study, MION-MPS was first synthesized via surface modification of MION using MPS in order to introduce the vinyl group onto the surface of MION. During surface modification, the hydroxyl groups on the surface of the MION reacted with the methoxy group of MPS, leading to

the addition of 3-methacryloyloxypropyl group onto the surface of MION through Si-O bonding (Figure 1). Then, MIP shell was fabricated through copolymerization of the acrylamide (monomer) and EGDMA (cross-linker) with BPO and SDZ as the radical initiator and template, respectively. The surface modification of MION and MIP shell fabrication were confirmed using IR spectroscopy (Figure 2A). For MION, an intense peak at 583 cm^{-1} was attributed to Fe-O. For MION-MPS, a few new absorption peaks appeared in the range of 800–1700 cm^{-1}. The characteristic peaks of the Si-O-Si group appeared at about 1018 cm^{-1} and the carbonyl group at 1717 cm^{-1}. These peaks indicated that MPS was successfully grafted onto the surface of MION. In addition, the peak at around 2934 cm^{-1} was attributed to C-H stretching. This peak further showed the presence of MPS on the MION. For MION-MIP, the peaks around 2980 and 1725 cm^{-1} were more intense. This result indicated the presence of the MIP shell on MION. Also, the peak at 1717 cm^{-1} was shifted to 1725 cm^{-1}, indicating the formation of a polymer through the reaction between the double bond of acrylamide and vinyl groups of MPS.

The result from the TGA showed that the weight loss for MION-MPS was greater than that for MION (Figure 2B). This result indicated that MPS was successfully added onto the surface of MION. MION-MIP showed the greatest weight loss as compared to MION and MION-MPS. This result showed that polymerization was successfully imprinted onto the surface of MION-MPS. The size and shape of MION-MPS and MION-MIP were examined by the SEM technique. It was observed that the diameter of MION and MION-MPS was about 10 nm (Figure 2Ci and 2Cii). As reported by Tay et al. (22), the morphology of MION is not influenced by the surface modification of MION by using silane derivatives. After the formation of MIP, the diameter of MION-MIP was increased to about 100 nm (Figure 2Ciii).

3.2 Binding properties

3.2.1 Adsorption kinetic studies of MION-MIP and MION-NIP

According to Kong et al. (3), the adsorption of sulfonamides in acetonitrile produced the highest adsorption capacity, whereas the presence of water and methanol can disturb the binding effect of the magnetic MIPs by destroying the hydrogen bond. Therefore, in this study, all adsorption experiments were carried out in acetonitrile in order to evaluate the performance of the synthesized MION-MIP. An adsorption kinetics test was carried out to study the adsorption capacity of MION-MIP and MION-NIP with adsorption time (Figure 3A). The result showed that the MION-MIP showed a fast adsorption rate in the first 150 s and then increasing slightly to reach equilibrium after 400 s. This was probably due to the template molecules that were captured in the cavities on the surface of the polymer at the first stage and after most of the cavities were occupied, the target molecules had to be penetrated into the deeper part of the polymer, which would be more time consuming (3). Moreover, the maximum adsorption capacity of MION-MIP toward SDZ was found to be three times higher than that of MION-NIP. This result showed the contribution of the cavities of MIP to the adsorption of template molecules.

3.2.2 Binding isotherm

The binding isotherm of MION-MIP and MION-NIP was determined using SDZ solutions with the concentration ranging from 0.5 to 30 μg ml^{-1}. The amount of SDZ bound to MION-MIP increased sharply with increasing SDZ concentration from 0.5 to 20 μg ml^{-1} (Figure 3B). However, the curve was

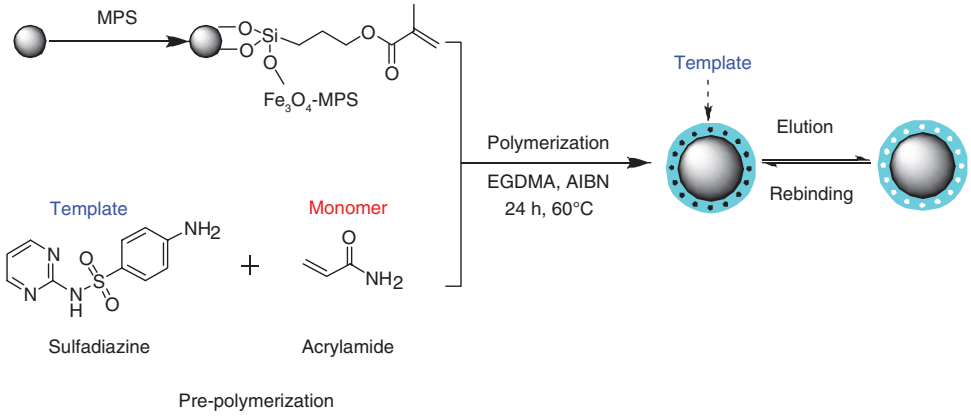

Figure 1: Schematic diagram for MION-MIP synthesis.

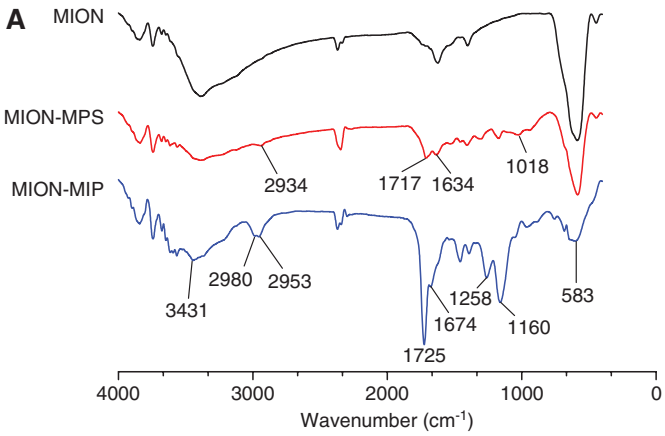

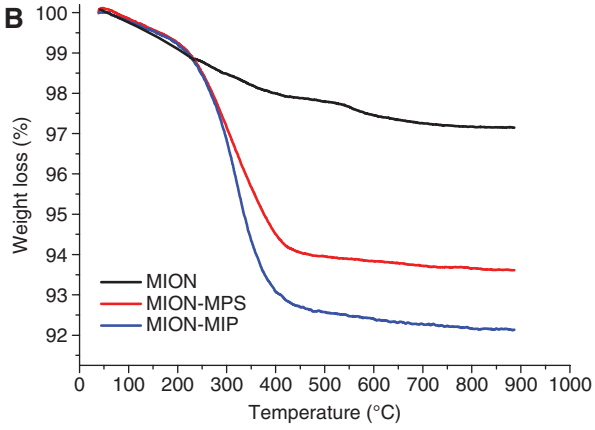

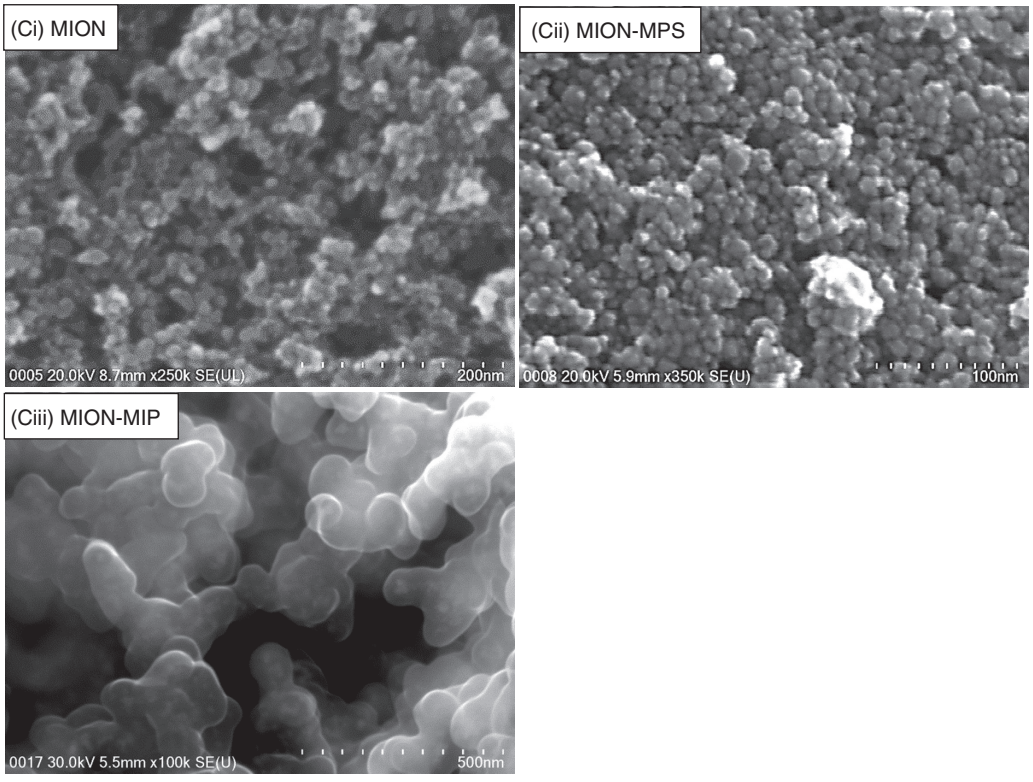

Figure 2: Characterization of MION, MION-MPS, and MION-MIP.
(A) FTIR spectra recorded from 4000 to 400 cm^{-1}; (B) TGA curves; (C) SEM image of MION-MPS and MION-MIP.

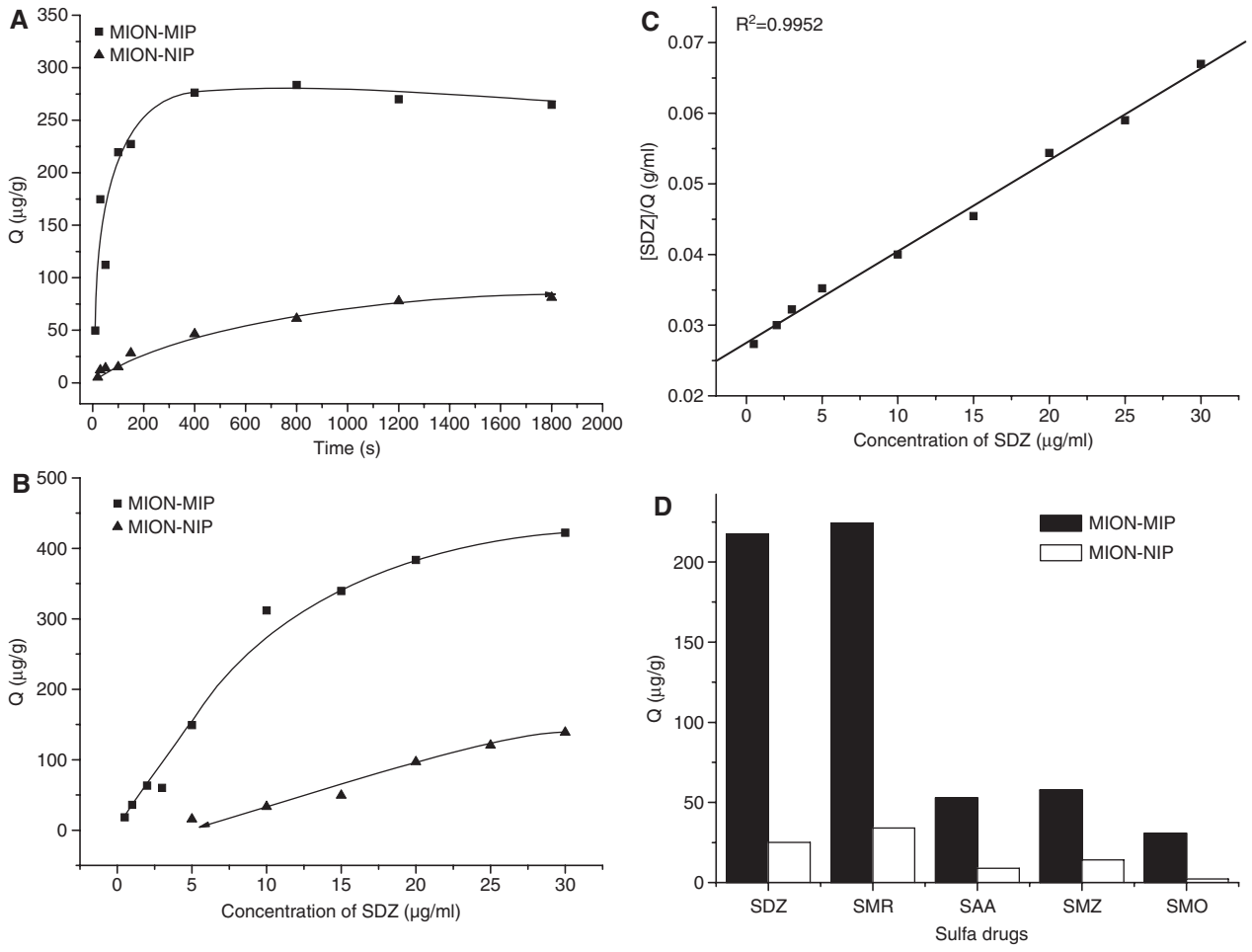

Figure 3: (A) Adsorption dynamic curves of MION-MIPs and MION-NIPs. (B) Adsorption isotherm of SDZ onto MION-MIPs and MION-NIPs. (C) Langmuir plot to estimate the binding mechanism of MION-MIPs toward SDZ. (D) Adsorption capacity of MION-MIP and MION-NIP toward SDZ, SMR, SAA, SMZ, and SMO.

flattening after the concentration of SDZ was >20 μg ml^{-1}. The MION-NIP curve also showed an increasing tendency; however, the adsorption ability is not so obvious. Apparently, MION-MIP possessed a higher loading ability toward the template as compared to the MION-NIP. The result suggested that the existence of imprinting cavities differentiated the binding ability of MION-MIP as compared to MION-NIP. To further study the binding mechanism of SDZ onto the MION-MIP, Langmuir analysis was performed by using data of the binding isotherm. The equation for Langmuir adsorption isotherm model is as follows (3):

$$\frac{[\mathrm{SDZ}]}{Q}=\frac{1}{Q_{MAX}K_D}+\frac{[\mathrm{SDZ}]}{Q_{MAX}},$$

where Q represents the amount of SDZ bound to MION-MIP, K_D is the dissociation constant, Q_{MAX} represents the apparent maximum adsorption capacity, and [SDZ] is the free SDZ concentration at equilibrium. The value of K_D and Q_{MAX} can be obtained from the slope and intercept of Figure 3C. The result showed that the experimental data were fitted to Langmuir adsorption isotherm model with the correlation coefficient (R^2) of 0.9952. Therefore, based on the Langmuir adsorption isotherm model, the adsorption of SDZ occurred uniformly on the active site of the MION-MIP. Once the SDZ occupied the active site, no further adsorption could take place at this site. According to the slope and intercept of Figure 3C the Q_{MAX} and K_D of the high-affinity sites were 775 μg g^{-1} and 0.047 μg ml^{-1}, respectively. The Q_{MAX} obtained from this study was almost two times larger than the Q_{MAX} value obtained by Kong et al. (3) from the adsorption of SMR by using core-shell MIP. This result might be due to the smaller size of MION-MIP, which provided a larger surface area for the adsorption of template molecule.

3.2.3 Selective adsorption of MION-MIP and binding mechanism

The competitive binding test was applied to determine selectivity of MION-MIP toward the adsorption of SDZ. Five sulfonamides (SDZ, SMR, SAA, SMZ, and SMO) were selected for this study. As shown in Figure 3D, the adsorption of MION-MIP toward SDZ and SMR was dramatically higher than that toward SAA, SMZ, and SMO. However, the adsorption of MION-MIP toward SMR was found to be slightly higher than that toward the template (SDZ). To further investigate the root reason for such a result, computational modeling was carried out to imitate the molecular interactions between the monomer and SDZ and SMR.

It has been reported that the adsorption of template molecule by MIP mimics the natural recognition pathways of natural recognition elements such as enzymes (23). Therefore, the optimized structures between the selected sulfonamides and acrylamide (AA) are expected to mimic the interaction of SMO with dihydropteroate synthase found in the protein databank (Figure 4A). The X-ray crystal structure of dihydropteroate synthase-SMO complex (PDB ID: 3TZF) shows that SMO was bound to two amino acids [serine (SER) and threonine (THR)] through hydrogen bonding at the sulfonyl and amine group of SMO. Presumably, SDZ and SMR also have a relatively similar interaction pattern as THR and SER with SMO in the dihydropteroate synthase-SMO complex; the calculation was focused at the AA1 and AA2 positions, as indicated in Figure 4B and C.

The interaction energy between SDZ and SMR with acrylamide was compared with three different levels of calculations (Table 1). SMR had a slightly stronger interaction with acrylamide than SDZ (template) by about 3.50 kcal mol^{-1} with PM3, and almost the same interaction with the HF and DFT method. With B3LYP, the binding energies between SDZ and SMR with monomers were slightly different by 0.29 kcal mol^{-1}. The interaction energies between AA1 and SDZ were also very similar to SMR, which are -133.30 and -132.07 kcal mol^{-1}, respectively. However, the interaction energies between AA2 and the selected sulfonamides were slightly higher by about 3.04 and 3.37 kcal mol^{-1} with HF and B3LYP, respectively. From this result, acrylamide at AA2 position bound stronger than that at AA1, and contributed to SDZ and SMR recognition. Based on the optimized structures, the interaction energy between the template and each monomer was investigated by scanning the distance of AA1 and AA2 along the O···H distance for SDZ and SMR (Figure 5). The lowest point in the graph represents the lowest interaction

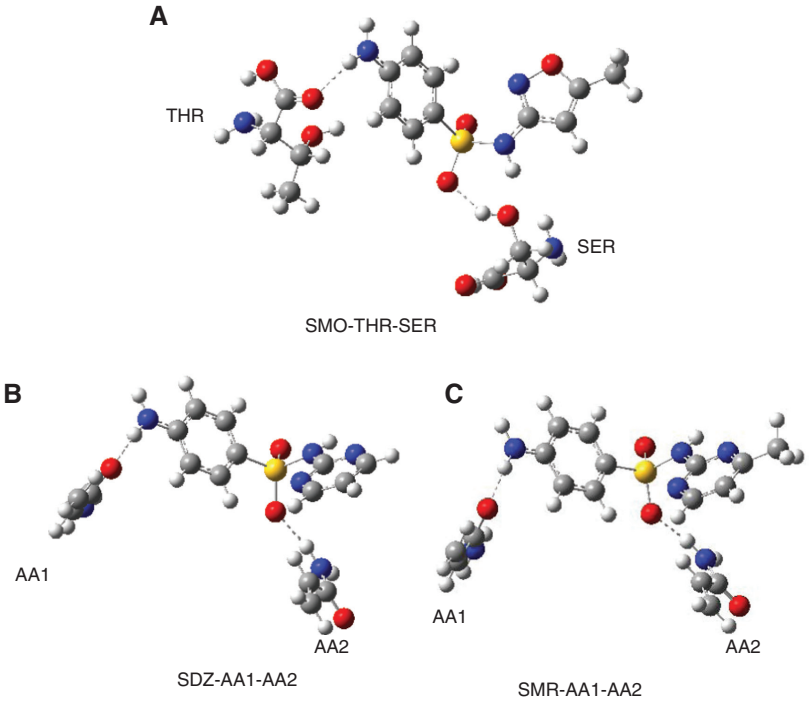

Figure 4: The interaction between the template and the monomer in comparison of the crystal structure of sulfonamide drug (SMO) from the protein database (PDB ID=3TZF).
The dashed line shows the hydrogen bonding interaction.

Table 1: The interaction energy between the templates and monomers with three different basis sets calculations.

Complex		Interaction energy (kcal mol^{-1})		
		PM3	HF/6-31G(d)	DFT/B3LYP/6-31G(d)
SDZ-AA1-AA2	ESDZ/AA1-AA2	-92.19	-150.95	-137.20
	ESDZ-AA2/AA1	-86.77	-147.02	-133.30
	ESDZ-AA1/AA2	-92.75	-159.34	-143.96
SMR-AA1-AA2	ESMR/AA1-AA2	-95.69	-150.72	-137.49
	ESMR-AA2/AA1	-89.28	-144.92	-132.07
	ESMR-AA1/AA2	-97.53	-162.38	-147.23
SMO-THR-SER	ESMO/THR-SER	-211.87	-661.36	-641.99
Relative interaction energy between SDZ and SMR with monomers	ESDZ/AA1-AA2-ESMR/AA1-AA2	3.50	-0.23	0.29
Relative interaction energy between SDZ and SMR with AA1	ESDZ-AA2/AA1-ESMR-AA2/AA1	2.51	-2.10	-1.23
Relative interaction energy between SDZ and SMR with AA2	ESDZ-AA1/AA2-ESMR-AA1/AA2	4.78	3.04	3.27

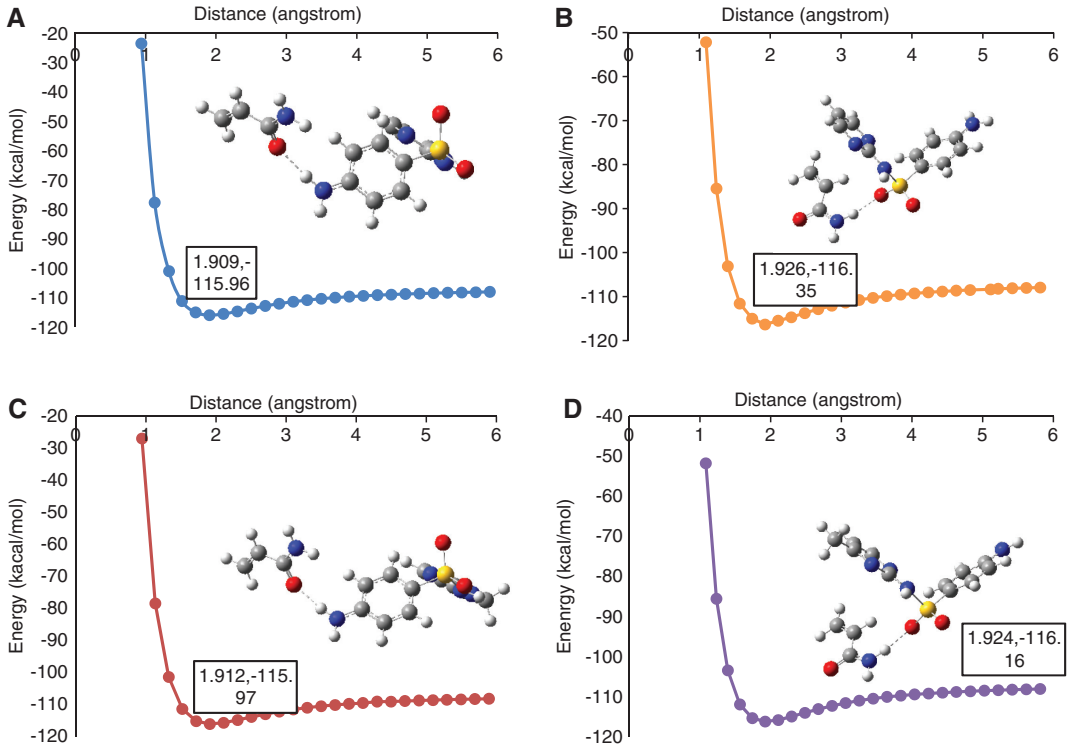

Figure 5: Interaction energy plotted against the O-H distance for (A) SDZ and AA1, (B) SDZ and AA2, (C) SMR and AA1, and (D) SMR and AA2.

energy structure, and the interaction between the SDZ and SMR with the monomer was similar to each other. Thus, SDZ and SMR can bind to MION-MIP through a similar interaction during the extraction process.

Another possible reason for the poor recognition toward these two sulfonamides might be due to the smaller size effect of MION-MIP, which creates the larger absorption surface area for the template. Besides the interaction energy and surface effect, the swelling behavior, which depends on the solvents, as reported by Koohpaei et al. (24) and Faizal et al. (25), would also cause the difference in the three-dimensional configuration of the functional groups that result in poorer capacity for site recognition between SDZ and SMR.

4 Conclusion

In this work, MION-MIP was prepared for the recognition and extraction of SDZ. By imprinting the acrylamide-based MIP onto the MPS-modified MION, the size of MION-MIP was around 100 nm. The result showed that the obtained MION-MIP possessed fast adsorption kinetics with only 400 s to reach equilibrium. The maximum adsorption capacity of MION-MIP was 775 μg g^{-1}. The results from the competitive binding test indicated that the adsorption of MION-MIP toward SDZ and SMR was dramatically higher than that toward other selected sulfonamides. The result from the interaction energy calculation showed that the energies between SDZ and SMR are similar and could have the same binding property in the MION-MIP.

Acknowledgments: We thank the Ministry of Education Malaysia (ERGS-Project no. ER005-2013A) and the University of Malaya (UMRG- RP020C-14AFR and RP001C-13ICT) for financial support.

References

1. García-Galán MJ, Díaz-Cruz MS. Identification and determination of metabolites and degradation products of sulfonamide antibiotics. TrAC-Trend Anal Chem. 2008;27:1008–22.
2. Msagati TAM, Nindi MM. Multiresidue determination of sulfonamides in a variety of biological matrices by supported liquid membrane with high pressure liquid chromatography-electrospray mass spectrometry detection. Talanta. 2004;64:87–100.
3. Kong X, Gao R, He X, Chen L, Zhang Y. Synthesis and characterization of the core-shell magnetic molecularly imprinted polymers (Fe_3O_4@MIPs) adsorbents for effective extraction and determination of sulfonamides in the poultry feed. J Chromatogr A. 2014;1245:8–16.
4. Mohanta T, Goel S. Prevalence of antibiotic-resistant bacteria in three different aquatic environments over three seasons. Environ Monit Assess. 2014;186:5089–100.
5. Sidrach-Cardona R, Hijosa-Valsero M, Marti E, Balcázar JL, Becares E. Prevalence of antibiotic-resistant fecal bacteria in a river impacted by both an antibiotic production plant and urban treated discharges. Sci Total Environ. 2014;488–489:220–7.
6. Vasapollo G, Sole RD, Mergola L, Lazzoi MR, Scardino A, Scorrano S and Mele G. Molecularly imprinted polymers: present and future prospective. Int J Mol Sci. 2011;12:5908–45.
7. Bakas I, Oujji NB, Istamboulié G, Piletsky S, Piletska E, Ait-Addi E, Ait Ichou I, Noguer T, Rouillon R. Molecularly imprinted polymer cartridges coupled to high performance liquid chromatography (HPLC-UV) for simple and rapid analysis of fenthion in olive oil. Talanta. 2014;125:313–8.
8. Cheng W, Ma H, Zhang L, Wang Y. Hierarchically imprinted mesoporous silica polymer: an efficient solid-phase extractant for bisphenol A. Talanta. 2014;120:255–61.
9. Xu S, Lu H, Chen L. Double water compatible molecularly imprinted polymers applied as solid-phase extraction sorbent for selective preconcentration and determination of triazines in complicated water samples. J Chromatogr A. 2014;1350:23–9.
10. Du B, Qu T, Chen Z, Cao X, Han S, Shen G, Wang L. A novel restricted access material combined to molecularly imprinted polymers for selective solid-phase extraction and high performance liquid chromatography determination of 2-methoxyestradiol in plasma samples. Talanta. 2014;129:465–72.
11. Urraca JL, Castellari M, Barrios CA, Moreno-Bondi MC. Multiresidue analysis of fluoroquinolone antimicrobials in chicken meat by molecularly imprinted solid-phase extraction and high performance liquid chromatography. J Chromatogr A. 2014;1343:1–9.
12. Braga LR, Rosa AA, Dias ACB. Synthesis and characterization of molecularly imprinted silica mediated by Al for solid phase extraction of quercetin in *Ginkgo biloba* L. Anal Method. 2014;6:4029–37.
13. Scorrano S, Mergola L, Sole RD, Lazzoi MR, Vasapollo G. A molecularly imprinted polymer as artificial receptor for the detection of indole-3-carbinol. J Appl Polym Sci. 2014;131:40819.
14. Wulandari M, Urraca JL, Descalzo AB, Amran MB, Moreno-Bondi MC. Molecularly imprinted polymers for cleanup and selective extraction of curcuminoids in medicinal herbal extracts. Anal Bioanal Chem. 2015;407:803–12.
15. Xie L, Guo J, Zhang Y, Shi S. Efficient determination of protocatechuic acid in fruit juices by selective and rapid magnetic molecular imprinted solid phase extraction coupled with HPLC. J Agr Food Chem. 2014;62:8221–8.
16. Sun X, Wang J, Li Y, Yang J, Jin J, Shah SM, Chen J. Novel dummy molecularly imprinted polymers for matrix solid-phase dispersion extraction of eight fluoroquinolones from fish samples. J Chromatogr A. 2014;1359:1–7.
17. Sobiech M, Zolek T, Lukiński P, Maciejewska D. A computational exploration of imprinted polymer affinity based on voriconazole metabolites. Analyst 2014;139:1779–88.
18. Basozabal I, Gomez-Caballero A, Diaz-Diaz G, Guerreiro A, Gilby S, Goicolea MA, Barrio RJ. Rational design and chromatographic evaluation of histamine imprinted polymers optimized for solid-phase extraction of wine samples. J Chromatogr A. 2013;1308:45–51.
19. Lakshmi D, Akbulut M, Ivanova-Mitseva PK, Whitcombe MJ, Piletska EV, Karim K, Güven O, Piletsky SA. Computational design and preparation of MIPs for atrazine recognition on a conjugated polymer-coated microtiter plate. Ind Eng Chem. 2013;52:13910–6.
20. Abdin MJ, Altintas Z, Tothill IE. *In silico* designed nanoMIP based optical sensor for endotoxins monitoring. Biosens Bioelectron. 2015;67:177–83.
21. Karaagac O, Kockar H, Beyaz S, Tanrisever T. A simple way to synthesize superparamagnetic iron oxide nanoparticles in air atmosphere: iron ion concentration effect. IEEE T Magn. 2010;46:3978–83.
22. Tay KS, Rahman NA, Abas MRB. Magnetic nanoparticle assisted dispersive liquid-liquid microextraction for the determination of 4-nnonylphenol in water. Anal Methods. 2013;5:2933–8.
23. Kryscio DR, Peppas NA. Critical review and perspective of macromolecularly imprinted polymers. Acta Biomater. 2012;8:461–73.

24. Koohpaei AR, Shahtaheri SJ, Ganjali MR, Forushani AR, Golbabaei F. Application of multivariate analysis to the screening of molecularly imprinted polymers (MIPs) for ametryn. Talanta. 2008;75:978–86.

25. Faizal CKM, Kikuchi Y, Kobayashi T. Molecular imprinting targeted for α-tocopherol by calix[4]resorcarenes derivative in membrane scaffold prepared by phase inversion. J Membr Sci. 2009;334:110–6.